



Parametric Study of combined cycle power plant by Energy and Exergy Analysis located in Iran

Hamid Hassanzadeh Afrouzi ¹, Hossein Zare Valokolaei ², Seyyed Mostafa Seyyedi ^{3*}

^{1,3} Department of Mechanical Engineering, National University of Skills (NUS), Tehran, Iran

² Department of Chemical Engineering, Buein Zahra Technical University, Buein Zahra, Qazvin, Iran

ARTICLE INFO

Article Type:
Original Research

Received: 06.11.2025
Revised: 08.26.2025
Accepted: 10.21.2025

Keyword:
Power plant
Exergy
Energy
Power output
Electric efficiency

***Corresponding Author:**
Seyyed Mostafa Seyyedi
Email:
mostafa_5054@yahoo.com

ABSTRACT

In the present study, energy and exergy analysis of Neka combined cycle power plant in the north of Iran is carried out at minimum (220MW) and maximum (440MW) loads. With four units of 440MW, this power plant can produce 1760MW power. The effects of different parameters, including the outlet water sub-cooled temperature of condenser, ambient temperature, excess air, removing heaters, and sea temperature on power plant gross and net outputs and gross and net electric efficiencies, are examined. The obtained results show that the boiler accounts for the most exergy losses among the cycle components, showing a significant difference compared to the others. Moreover, it was found that the effect of sea temperature is significant as for one degree of rising seawater temperature, the plant output power and cycle efficiency decrease by 1459 kW and 0.156%, respectively. Also, the optimal excess air corresponds to the maximum level at minimum load and the minimum level at maximum load. The results show that by augmenting the excess air from 0 to 25%, the gross power output reduces by about 2500 kW.



Introduction

Optimizing power generation has become essential due to rising energy costs and dwindling fossil fuel supplies. Combined cycle power plants (CCPPs) offer improved efficiency over separate gas and steam cycles. Exergy analysis, grounded in both thermodynamic laws, identifies system inefficiencies by evaluating energy quality and the theoretical maximum work extractable from energy sources. Exergy represents the maximum useful work a system can deliver when approaching equilibrium with its surroundings. Unlike energy, it is destroyed in real processes, making exergy analysis an effective tool for identifying inefficiencies in power systems [1]. Many researchers have recently studied the exergy analysis of combined cycles [2-4].

Mokhtari et al. [5] applied thermo-economic and advanced exergy analyses to CCPPs, identifying turbine inlet temperature and compressor ratio as key factors in improving efficiency and reducing exergy losses. Afterward, Ahmadi and Toghraie [6] showed that in a 200 MW Iranian power plant, the condenser and boiler account for the highest energy and exergy losses, respectively. Additionally, Pattanayak et al. [7] demonstrated that increasing inlet air temperature and pressure losses negatively impacts CCPP efficiency and output, underlining the importance of optimal operating conditions.

Then, Aliyu et al. [8] evaluated the performance of a 747 MW combined cycle power plant with a triple-pressure heat recovery steam generator (HRSG), revealing that combustion chambers were the primary sources of exergy destruction, while condensers accounted for the highest energy losses. The plant achieved energy and exergy efficiencies of 59.12% and 58.24%, respectively. Aliyu et al. [9] analyzed a reheat configuration and identified the stack and high-pressure evaporator as the main contributors to irreversibility. Their findings emphasized that operational parameters such as superheat and reheat pressures, along with steam quality, play a crucial role in improving thermal efficiency and optimizing overall plant performance. Omidpanah et al. [10] simulated the parameters affecting the production capacity and efficiency of a combined cycle power plant unit. The ANSALDO unit of Yazd combined cycle power plants was therefore modeled and examined. Their findings show that each gas unit of this power plant had a thermal efficiency of 34% and a production capacity of 134 MW. When these units were coupled to the steam unit in the design, the total thermal efficiency of the power plant reached 50% and its production capacity reached 422 MW.

Anetor et al. [11] conducted classical and advanced exergy analyses of a 750 MW steam power plant, identifying the condenser and boiler as primary sources of exergy destruction. Although a significant portion of irreversibility was

unavoidable, reducing endogenous losses in turbines and boilers could improve efficiency by 2.5%. Altarawneh et al. [12] examined a 400 MW natural gas/diesel hybrid CCPP in Jordan and highlighted major performance losses due to irreversibilities in gas and steam turbines. Their findings emphasized optimization potential in energy-constrained regions. Elwardany et al. [13] investigated a 750 MW CCPP in Egypt and found combustion chambers and HRSGs to dominate exergy destruction, suggesting that targeted improvements in these components can significantly enhance overall plant efficiency and sustainability.

Omara et al. [14] conducted advanced exergy analysis of Sudan's 180 MW Garri "1" CCPP, identifying combustion chambers and stacks as major sources of exergy and energy losses. Their results showed only 3% efficiency improvement potential, indicating high irreversibility in thermal-dependent systems. In another study, Prakash and Singh [15] analyzed a combined cycle power plant retrofitted with carbon capture and utilization. The gas turbine got 96.66% exergy efficiency at 12.7 pressure ratio and 1475 K turbine inlet temperature; the combustion chamber showed the highest exergy destruction (12.7 cycle pressure ratio, 1400 K). These findings provide valuable insights for assessing and optimizing the performance of conventional and carbon capture-integrated combined cycle configurations.

Abdulsitar et al. [16] analyzed a 1500 MW combined cycle power plant in Erbil using energy and exergy methods. Their study showed significant improvements in overall efficiency following conversion to combined cycle operation, with condensers and combustion chambers identified as the main sources of energy and exergy losses, respectively. The effect of environmental conditions and fuel type on the energy and exergy parameters of a steam power plant have been studied by Babaei et al. [17]. In their research, the effect of natural gas extracted in various regions of Iran, including Khangiran, Kangan, Pars, Bidboland, Ahvaz and Sarakhs on Ramin Ahvaz steam power plant was investigated. Investigating the increase in temperature from 5 to 40 °C showed that the net power output of the power plant decreases to 14 MW and of the exergy destruction rate in the condenser increases to 16 MW. At 25 °C, the maximum exergy destruction rate is related to Bidbland region with 500 MW and the lowest rate is related to Sarakhs region with 370 MW.

Ibrahim et al. [18] proposed a statistical modeling approach to evaluate gas turbine performance using response surface methodology (RSM) and central composite design (CCD). Their model demonstrated excellent agreement with simulation data ($R^2 \approx 0.985$) and was successfully validated using operational data from the MARAFIQ combined cycle power plant. This methodology offers a

reliable tool for performance prediction and system optimization, enabling better understanding of gas turbine behavior under various operating conditions in complex power generation systems. Ibrahim et al. [19] have been carried out thermodynamic modeling of various gas turbine configurations using MATLAB, assessing the effects of ambient and turbine inlet temperatures on plant performance. Their analysis identified the intercooler–regenerative–reheat configuration as offering the highest thermal efficiency, which declined as ambient temperature increased. They also found that parameters such as compression ratio, turbine inlet temperature, and air-to-fuel ratio significantly influence thermal efficiency.

Kazemian and Gandjalikhan Nassab [20] performed a thermodynamic and statistical analysis of gas turbine cycle performance using response surface methodology (RSM) based on central composite design (CCD). Their study evaluated key operational and design parameters, including turbine and compressor inlet temperatures, combustion chamber pressure drop, fuel quality, and air mass flow rate. The developed regression models predicted thermal efficiency and net power output with an inaccuracy margin below 5.5%. Under optimal conditions, the gas turbine cycle achieved a thermal efficiency of 45.71% and a net power output of 4.182 MW, demonstrating the accuracy and usefulness of the proposed modeling approach.

Alnaimi et al. [21] conducted a parametric study on combustion process optimization in an aging gas turbine plant (two Siemens V94.2 units) under current operational conditions. Their findings indicated that thermal efficiency increased with lower compressor inlet temperature and higher compression ratio, reaching a maximum of 30% efficiency and 140 MW output. Wang et al. [22] performed multi-objective optimization of a gas turbine combined cycle system by integrating energy, economic, and environmental criteria. Using a genetic algorithm, their analysis revealed significant improvements in exergetic efficiency and reductions in CO₂ emissions and annual costs. Among various factors, natural gas pricing was found to have the greatest influence on overall economic performance, surpassing even environmental and non-energy costs in impact.

Elwardany et al. [23] performed an exergy analysis of a gas turbine power plant situated in Assiut, Egypt, operating under high-temperature conditions. They evaluated the performance of the simple gas turbine cycle and identify the sources of thermodynamic inefficiencies using the second law of thermodynamics as a basis for analysis. To this end, they concentrated on how different ambient temperature affected the exergy efficiency, exergy destruction, and net power production of the cycle. Their results showed that higher

temperatures cause more exergy loss, which lowers efficiency and net power output. Thus, minimizing the negative consequences of hot weather circumstances depends on improving the architecture of the combustion chamber. Kamali et al. [24] has conducted energy and exergy studies of a direct solar steam power plant with solar parabolic for Yazd city including many water preheaters. In this study, for different cases in which the cycle has up to 4 preheaters, the efficiency of the first and second laws of thermodynamics was investigated. In the case of 4 preheaters, based on obtained results, it was revealed that the efficiency of the first and second laws were 17.2% and 16%, respectively which was a significant increase compared to the case where the cycle had one, two or three preheaters.

The above literature highlights extensive global efforts to evaluate thermal power plants using energy and exergy analyses. A recurring finding is the significant role of boiler performance in determining overall CCPP efficiency. This study aims to investigate the effects of condenser outlet temperature under minimum and maximum load conditions on boiler behavior, using ThermoFlow 19 for detailed simulation. As nuclear energy is phased out and renewable integration slows, combined cycle power plants can serve as a transitional technology toward sustainable energy. Despite numerous global studies, no detailed performance analysis has been conducted for a large-scale plant under actual Iranian climatic conditions. This work provides a quantitative assessment of how sea temperature and excess air affect power output and efficiency in a coastal CCPP in Iran, while also offering insight into performance improvement strategies under real operational scenarios. The novelty of the present study lies in performing a detailed parametric analysis of the 1760 MW Neka combined cycle power plant under real climatic conditions. Unlike previous works, this study specifically examines the combined effects of seawater temperature, excess air variation, and heater removal, providing practical insights for improving the efficiency of large-scale coastal CCPPs.

Neka power plant specification

The Shahid Salimi Neka power plant, located in northern Iran, consists of four 440 MW combined cycle units with a total capacity of 1760 MW. Natural gas is used as the primary fuel, with Mazut as a backup. Process water is extracted from three deep wells, and seawater is used for cooling. The once-through boiler, featuring a two-stage furnace design, produces superheated steam via radiative heat transfer. The steam passes through high, intermediate, and low-pressure turbine sections, followed by condensation and feedwater preheating using seven heaters. The turbine operates under variable pressure, depending on load.

Plant analysis is performed at two load levels: 220 MW (minimum) and 440 MW (maximum). A schematic of the system and simulation setup is shown in Fig. 1.

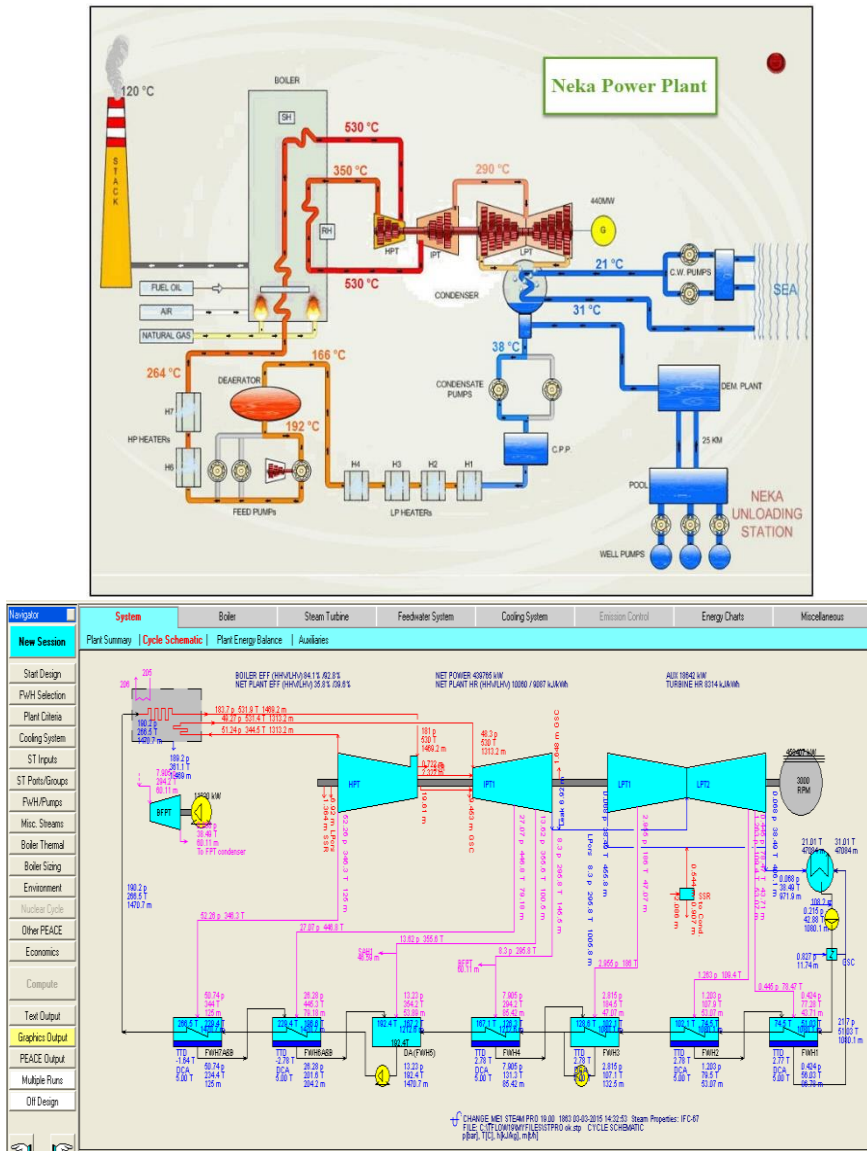
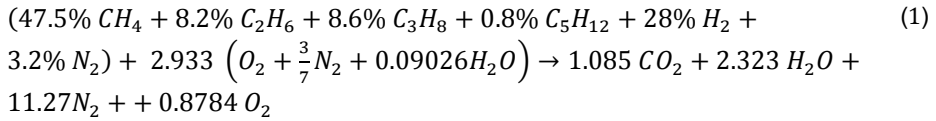


Figure 1. A schematic diagram of Neka CCPP [25] and its model in thermoflow software.

Exergy analysis

Exergy in thermodynamic systems consists of two main components: physical and chemical exergy. In combustion processes, chemical exergy reflects the deviation of a substance's composition from environmental equilibrium and

plays a dominant role. In this study, exergy analysis considers a combustion scenario with 20% excess air and 60% relative humidity, for which the fuel-air reaction is balanced as presented in the following equation.



The thermomechanical exergy of combustion gases at the stack temperature is defined as follows:

$$\varphi_{ph} = \sum_{i=1}^n y_i \left[h_{i,T} - h_{i,T_0} - T_0 (s_{i,T}^0 - s_{i,T_0}^0) + RT \ln \frac{p}{p_0} \right] \quad (2)$$

The following equation also defines the chemical exergy of combustion gases:

$$\varphi_{ch} = RT_0 \sum_{i=1}^n N_i \ln \frac{p_{i,0}}{p_{i,00}} = RT_0 \sum_{i=1}^n N_i \ln \frac{y_{i,0}}{y_{i,00}} \quad (3)$$

The total exergy is calculated from the summation of thermomechanical and chemical exergy. This value is the exergy of a boiler stack that can be recovered. The ratio of exergy loss of combustion gases to fuel exergy is:

$$\frac{\varphi_{Stack}}{\varphi_{chf}} = \frac{n_{gas}}{n_{fuel}} \times \frac{\varphi_{gas}}{\varphi_{chf}} \quad (4)$$

The chemical exergy of natural gas is calculated according to the percentage of its compounds, which is:

$$N_{fule} \times \varphi_{chf} \quad (5)$$

The lower heating value (LHV) for the natural gas due to its components is defined as follows:

$$LHV_{natural\ gas} = N_{fule} \times LHV \quad (6)$$

It has been assumed in this study that the kinetic and potential parts of exergy are negligible. The continuity, energy, and exergy equations for the volume control of various components of the cycle under steady-state conditions are defined as follows:

$$\sum m_i = \sum m_e \quad (7)$$

$$\dot{Q} - \dot{W} = \sum m_e h_e - \sum m_i h_i \quad (8)$$

$$X_{heat} - \dot{W} = \sum m_e \varphi_e - \sum m_i \varphi_i + i \quad (9)$$

The net exergy translated by heat Q at temperature T is calculated with the following equation:

$$X_{heat} = \sum \left(1 - \frac{T_0}{T}\right) Q \quad (10)$$

The total exergy is defined as the following correlation:

$$\varphi = h - h_0 - T_0(s - s_0) \quad (11)$$

which T_0 is the standard temperature at ambient temperature and h_0 and s_0 are enthalpy and entropy at T_0 . Due to the above correlation, the total exergy of the flow is as follows:

$$X = m \varphi = m [h - h_0 - T_0(s - s_0)] \quad (12)$$

Data analysis

Calculation of exergy of the gases from the fuel combustion

The primary fuel for the Neka combined power plant is natural gas. So the exergy analysis is carried out for this type of fuel. The natural gas components analysis to feed boilers is given in Table 1. The molar fraction of the air components under circumstances of 1 atmosphere and 60% relative humidity is shown in Table 2.

Table 1. The volume fraction of the natural gas components.

Componet of natural gas	Mole (%)	Mass (%)
Methane (CH ₄)	98.010	95.294
Ethane (C ₂ H ₆)	0.571	1.041
Propane (C ₃ H ₈)	0.136	0.363
i-Butane (i-C ₄ H ₁₀)	0.028	0.100
n-Butane (n-C ₄ H ₁₀)	0.083	0.291
i-Pentane (i-C ₅ H ₁₂)	0.017	0.074
n-Pentane (n-C ₅ H ₁₂)	0.018	0.079
n-Hexane and Heavier (C ₆ H ₁₄ ⁺)	0.092	0.483
Carbon dioxide (CO ₂)	0.517	1.379
Hydrogen sulfide (H ₂ S)		1.7 PPM
Nitrogen (N ₂)	0.894	0.894
Total	100.000	100.000

Table 2. Molar fraction of the air component.

Componet of natural gas	Molar fraction (%)
Nitrogen (N ₂)	76.62
Oxygen (O ₂)	20.55
Water (H ₂ O)	1.88
Carbon dioxide (CO ₂)	0.03
Others	0.92

The stack gas temperature of the Neka power plant is 120 °C with zero relative pressure, resulting in $\ln(p/p_0)$ is 0. Accordingly, the thermomechanical exergy of combustion gases is $\varphi_{ph} = 348.1615 \text{ kJ/kmol}$, and the chemical exergy is $\varphi_{ch} = 1752.77 \text{ kJ/kmol}$. Thus, the total exergy recoverable from the boiler stack is $\varphi_{tot} = 2100.9315 \text{ kJ/kmol}$. These values are obtained using standard thermodynamic property data as referenced in [11]. The chemical exergy of the natural gas fuel is also computed from its composition using Equation (3), yielding approximately $N_{fule} \times \varphi_{ch f} \cong 838799 \text{ kJ/kmol}$.

Calculation of LHV

The LHV of natural gas is calculated from its composition data using equation (6) and the standard thermodynamic properties of its components, assuming a gas density of 0.699 kg/m^3 . The resulting value is approximately $LHV_{natural\ gas} \cong 804601$, in accordance with thermodynamic data reported in [11].

Exergy analysis of the power plant components at the minimum load (220 MW)

Stack: as it was mentioned, the total exergy is calculated from summing the thermomechanical and chemical exergies, so the total exergy of the stack based on the equations (1) and (2) is $\varphi_{tot} = 2100.9315 \text{ kJ/kmol}$. The ratio of exergy loss of combustion gases to fuel exergy based on equations (4) is equal to 0.03167, so the exergy loss from the stack is $i_{stack} = 20477.18 \text{ kW}$.

Boiler: the efficiency of the first law of thermodynamic for the boiler is $\eta_{gen} = \frac{Output}{Input} = 83.2\%$, and the efficiency of the second law of thermodynamics is $\eta_{II} = \frac{m_s \varphi_{st}}{m_f \varphi_{CH}} = 39.67\%$. The ratio of total exergy losses of the boiler to the exergy of fuel chemicals is $I_{Boiler} = 1 - \eta_{II} = 0.6024$. Boiler total irreversibility magnitude is 397917.85 kW , and irreversibility magnitude in the combustion and heat transfer stage is $I_{ht+comb} = I_{Boiler} - I_{stack} = 377440.677 \text{ kW}$.

Turbine: the actual work of the H.P. turbine is $W_{act} = \Delta h = 321.404 \text{ kJ/kg}$. The exergy efficiency of the H.P. turbine is $\eta_{II} = \frac{W_{act}}{\varphi_{in}} = 92\%$. So the H.P. turbine irreversibility is $\varphi_{loss t} = \varphi_{in} - W_{act} = 24.96 \text{ kJ/kg}$. Finally, the H.P. turbine exergy loss is $i_t = m_s \times \varphi_{loss t} = 4694.47 \text{ kW}$. Based on the calculations for the H.P. turbine, the parameters for the I.P. turbine are $W_{act} = 74638.09 \text{ kW}$, $\eta_{II} = 94.3\%$, $i_t = 4509 \text{ kW}$. Similarly, these parameters for L.P. turbine are $W_{act} = 90497.77 \text{ kW}$, $\eta_{II} = 87.33\%$, $i_t = 13130.07 \text{ kW}$.

Condenser: the inlet exergy to the condenser based on equation (11) equals 26.79 kJ/kg . Also, the energy losses magnitude from the condenser is 279254 kW , which is 43% of the total energy entering the cycle. The condenser irreversibility is $i_c = m_s \times \varphi_{in} = 3354.3 \text{ kW}$.

Heaters: there are eight heaters in the cycle whose second law efficiencies and exergy losses are as follows. $\eta_{II(H1)} = 9.4\%$ and $i_{H1} = 101.66 \text{ kW}$, $\eta_{II(H2)} = 51.6\%$ and $i_{H2} = 1117.76 \text{ kW}$, $\eta_{II(H3)} = 78\%$ and $i_{H3} = 552.21 \text{ kW}$, $\eta_{II(H4)} = 86\%$ and $i_{H4} = 445.96 \text{ kW}$, $\eta_{II(H5)} = 84.15\%$ and $i_{H5} = 1067.9 \text{ kW}$, $\eta_{II(H6)} = 96\%$ and $i_{H6} = 772.14 \text{ kW}$, $\eta_{II(H7)} = 79.8\%$ and $i_{H7} = 1915 \text{ kW}$, $\eta_{II(H8)} = 92.3\%$ and $i_{H8} = 762.07 \text{ kW}$.

The efficiency of the first and second laws of thermodynamics of the cycle are $\eta_I = 35.62\%$ and $\eta_{II} = 34.41\%$, respectively.

Exergy analysis of the power plant components at the maximum load (440 MW)

Due to the similar formulas in this section and the previous, the results are only reported.

Stack: $\varphi_{tot} = 2100.9315 \text{ kJ/kmol}$, $\frac{\varphi_{Stack}}{\varphi_{chf}} = 0.06329$, $i_{stack} = 83845 \text{ kW}$.

Boiler: $\eta_{gen} = 80\%$, $\eta_{II} = 40.8\%$, $I_{Boiler} = 0.6535$.

The total irreversibility magnitude of the boiler is 865742 kW , and the irreversibility magnitude in the combustion and heat transfer stage is 781897 kW .

Turbine: $W_{act(HP)} = 295.95 \text{ kJ/kg}$, $\eta_{II(HP)} = 92.8\%$, $i_{t(HP)} = 8904 \text{ kW}$, $W_{act(IP)} = 152322.66 \text{ kW}$, $\eta_{II(IP)} = 94.42\%$, $i_{t(IP)} = 8997.13 \text{ kW}$, $W_{act(LP)} = 179201 \text{ kW}$, $\eta_{II(LP)} = 85.63\%$, $i_{t(LP)} = 30070 \text{ kW}$.

Condenser: The energy losses magnitude from the condenser is 519413 kW, which is 40% of the total energy entering the cycle. The condenser irreversibility is $i_C = 22031 \text{ kW}$.

Heaters: $\eta_{II(H1)} = 25\%$ and $i_{H1} = 83.4 \text{ kW}$, $\eta_{II(H2)} = 54.4\%$ and $i_{H2} = 2997.99 \text{ kW}$, $\eta_{II(H3)} = 89\%$ and $i_{H3} = 763.76 \text{ kW}$, $\eta_{II(H4)} = 90\%$ and $i_{H4} = 787.88 \text{ kW}$, $\eta_{II(H5)} = 85.8\%$ and $i_{H5} = 2494.44 \text{ kW}$, $\eta_{II(H6)} = 97.25\%$ and $i_{H6} = 1625.32 \text{ kW}$, $\eta_{II(H7)} = 89.82\%$ and $i_{H7} = 2441.11 \text{ kW}$, $\eta_{II(H8)} = 93.2\%$ and $i_{H8} = 1920.62 \text{ kW}$.

The efficiency of the first and second laws of thermodynamics of the cycle is $\eta_I = 34.54\%$ and $\eta_{II} = 33.3\%$ respectively. To summarize the above information, Figs. 2 and 3 show the exergy losses percentage of power plant cycle components and heaters, respectively. The boiler was found to have the highest exergy losses among all cycle components, primarily due to large temperature gradients during combustion, heat transfer limitations inherent in the one-pass Benson-type design, and the loss of high-temperature flue gases through the stack. These losses can be mitigated by optimizing burner design and combustion air preheating, implementing advanced excess air control to reduce stack losses without compromising combustion completeness, and improving heat recovery through multi-pressure heat recovery steam generators (HRSG) or optimized supplementary firing.

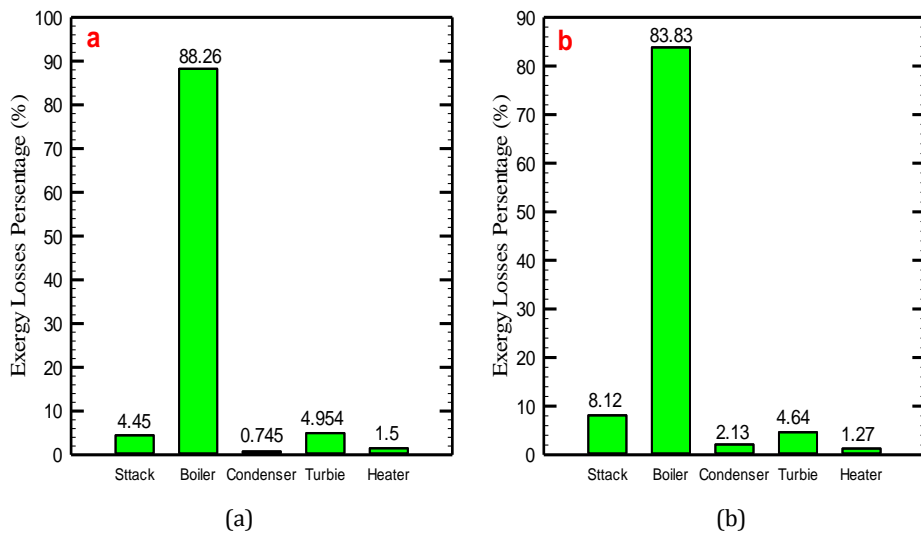


Figure 2. Exergy losses percentage of different components of the power cycle in (a) minimum load and (b) maximum load.

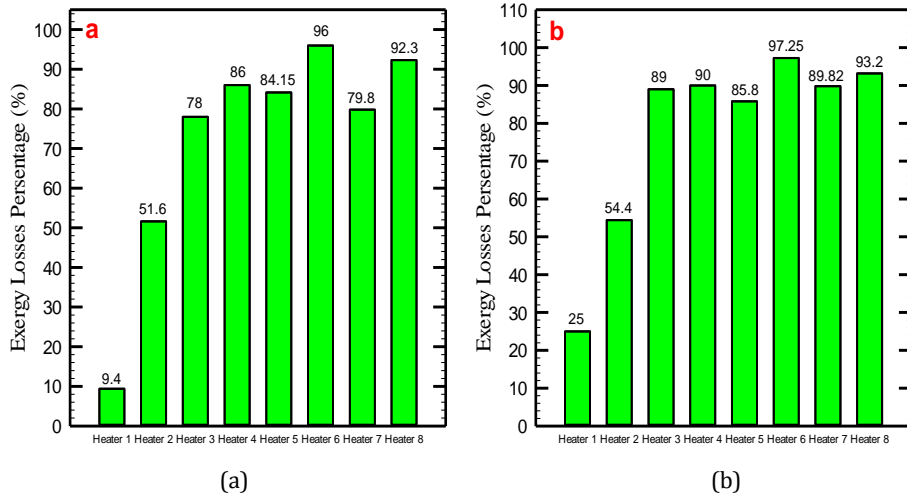


Figure 3. Exergy losses percentage of eight heaters of the power cycle in (a) minimum load and (b) maximum load

Result and discussion

Validation

In this study, advanced exergy analysis of a real CCPP was conducted, while conventional exergy analysis was employed to determine exergy destruction rates. The results were validated against the results of Ameri et al. [26]. As presented in Table 3, the calculated performance parameters exhibit a good agreement with those reported in [26].

Table 3. Comparison of the calculated values in the present study with the various previously reported values [26].

Performance parameters	Ref. [26]	Present Study
Heat Rate, HR	6.923	7.234
Heat to power ratio, HPR	1.082	1.031
Exhaust heat gas cycle, (MW)	287.81	296.73
CCPP thermal efficiency	52	55.1
CCPP exergetic efficiency	44.1	46.1
GT efficiency	31.1	32.8
ST efficiency	32.9	34.8

Outlet water sub-cooled temperature of the condenser

At this stage, the Thermo Flex module of the ThermoFlow software is employed to investigate the effects of outlet water sub-cooled temperature of the condenser on different parameters, including gross power, net power, net electric efficiency, and net heat rate. These effects are shown in Table 4 from the temperature of 0 °C (design state) to 6 °C in 13 cases. The first two rows of this table show that increasing the outlet water sub-cooled temperature of the condenser decreases the gross power and net power. Still, these reductions are subtle as the gross and net powers reduce by about 528 kW and 522 kW, respectively. Due to the constant flow rate and outlet temperature, by decreasing the outlet water sub-cooled temperature of the condenser, the inlet flow rate and temperature of the condenser decrease. Both of them lead to a reduction in power generation. The last two rows of this table show that by decreasing the outlet water sub-cooled temperature of condenser, net electric efficiency decreases, and net heat rate increases. In this case, also the insignificant variations are visible. Therefore, it can be concluded that changing the outlet water sub-cooled temperature of the condenser doesn't propose a critical factor for repowering the power plant.

Table 4. Effects of different outlet water sub-cooled temperature of condenser on various parameters.

Parameter	Unit	Case 1	Case 2	Case 3	Case 4	Case 5	Case 6	Case 7
Water-cooled condenser sub-cooling	°C	3	2.5	2	1.5	1	0.5	0
Gross power	kW	45093 3	45097 7	45102 1	45106 5	45111 0	45115 4	45119 8
Net power	kW	44079 6	44083 9	44088 3	44092 6	44097 0	44101 4	44105 8
Net electric efficiency	%	42.39	43.39	43.39	43.39	44.39	44.39	45.39
Net heat rate	kJ/kWh	9132	9131	9130	9129	9128	9127	9127

Parameter	Unit	Case 8	Case 9	Case 10	Case 11	Case 12	Case 14
Water-cooled condenser sub-cooling	°C	6	5.5	5	4.5	4	3.5
Gross power	kW	45067 0	450714	450757	450801	450845	450889
Net power	kW	44053 6	440580	440623	440666	440709	440752
Net electric efficiency	%	39.4	39.4	39.41	39.41	39.41	39.42

Net heat rate	kJ/kWh	9137	9136	9136	9135	9134	9133
---------------	--------	------	------	------	------	------	------

Air temperature and relative humidity

The air temperature and relative humidity are two parameters that can be changed both naturally affected by ambient and mechanically before entering the boiler to supply the combustion air. Their values are changed from minimum to maximum in a whole year to investigate the effects of these parameters. Based on the meteorological data, the ambient temperature ranges from 3°C to 34 °C, and relative humidity ranges from 60% to 96 %. The Steam Pro module from Thermoflow software is employed due to its higher compatibility to simulate the boiler. Increasing the ambient temperature enhances the boiler's temperature and flow rate of outlet gases. Fig. 4 displays the variations of boiler efficiency with ambient temperature. It shows that increasing the ambient temperature from 3°C to 34 °C enhances the boiler efficiency to about 1 % (from 92.01% to 93.17%).

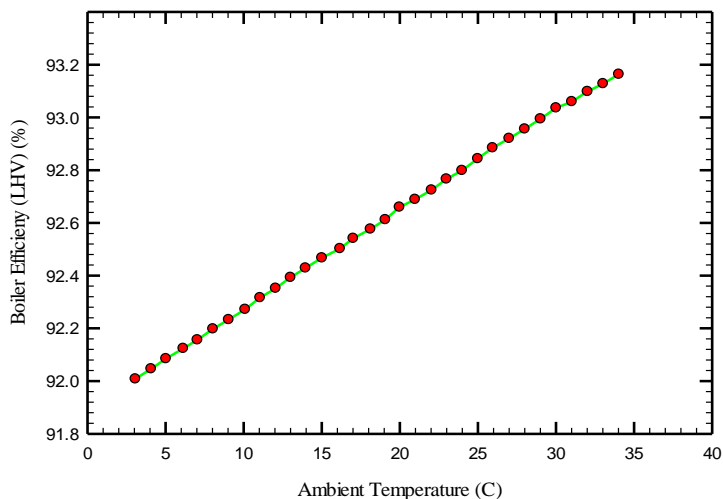


Figure 4. Variations of boiler efficiency with ambient temperature.

Figures 5 (a) and (b) present the variations of power plant gross output and net output with ambient temperature, respectively. The power plant's net output is produced in a turbine and influenced by the quality of the outlet steam. Due to the enhancement of boiler efficiency by increasing the inlet temperature to the cycle, the steam quality improves, and power net output increases. Fig. 4 also shows the augmentations of power net output by enhancing the ambient

temperature. The gross output power is defined as the power net output minus the domestic consumption of power plants such as pumps, fans, and so forth. So, by adding more air, the power net output increases, and the fans need to use more electricity. Hence, these changes cause some complexity in calculating the power gross output and fluctuations in Figure 3, which is insignificant.

Figures 5 (c) and (d) show the variations of plant net and gross electric efficiencies and plant net heat rate with ambient temperature. These figures illustrate that increasing the air temperature enhances the plant net and gross electric efficiencies and reduces the plant net heat rate. However, these changes are also subtle.

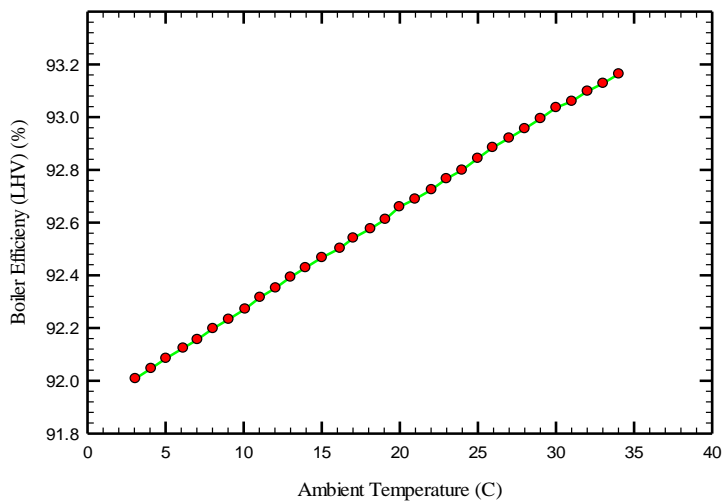


Figure 5. Effects of ambient temperature on the power plant (a) gross output, (b) net output, (c) gross and net electric efficiencies, and (d) net heat rate.

Percentage of excess air

The following four conditions are required fuel-burning completely:

- Enough air
- Complete mixing of air and fuel
- The furnace temperature is high enough to burn the inlet mixing air and fuel
- The furnace volume is such that there is enough time to complete the combustion reaction

Adjusting the correct amount of excess air will result in optimal combustion efficiency. CO_2 and O_2 in the combustion products represent the excess air. Increasing the extra air cause a reduction in loss due to incomplete combustion

but an enhancement in loss due to exiting the hot gas from the stack. So, to find the proper percentage of the excess air, these two parameters are needed to trade-off. To examine the effects of excess air on the main sections of the cycles, it ranges from 0 to 25 %. These effects are illustrated in Figure 6, which shows the variation of the net power plant output with respect to the excess air percentage. The results show that by increasing the percentage of the excess air, the boiler output temperature reduces, and the outlet gas flow rate increases, so that both of which are in accordance with the principles of combustion. Also, in the current simulation, only the excess air has changed, and other cycle parameters like temperature and outlet water flow rate of the boiler are presumed to be constant.

Consequently, increasing the excess air percentage reduces power output. Since the combustion is considered based on the spot analysis and the principles of thermodynamics, optimal circumstance corresponds to the combustion with no excess air. In addition, the fan's electricity consumption is enhanced by increasing the excess air and the flow rate of inlet and outlet gases. Since the net power is constant, the gross power decreases. On the other hand, the temperature of the smoke decreases by about 10 degrees. Because by increasing the combustion air, the flame temperature decreases according to the combustion diagram because the extra air also needs to receive heat from the environment to reach the flame temperature, which lowers the temperature of the smoke. Another reason is that by increasing inlet airflow, the work of the air heater also increases, which means that the inlet steam to this heat exchanger has increased. Instead of converting its energy to the power output, this vapor is used to heat the inlet air.

According to the software output, the cooling water flow rate of the cycle also decreases; about 12 t/h of additional steam in the air heater is used to heat the excess air, which means less vapor enters with the same amount the condenser. Still, since the pump, C.W., is steady, the use of this electric motor has not changed and thus does not affect efficiency.

Adding the excess air causes complete combustion and provides two fuel types with different heating values. It also results in various air, water, and fuel but constant boiler geometry in different loads. Increasing the amount of fuel and air changes the flame height. In low loads, the amount of fuel and air is low, and as a result, the flame height is low; thus, temperature increases in phase one of the boiler (saturated liquid phase). Since the Neka's boiler is one pass through Benson in type, the saturated water must be converted to saturated vapor at the end of phase one. Still, because of the improper flame height, the temperature doesn't rise enough in phase two, and inconsistency in the heat

transfer occurs, increasing the excess air solves this problem. In contrast, heat transfer in phase two (superheated) is well done in high loads because of high flame height. Then, if the percentage of excess air is high, the flame height increases too much, and the heat transfer in phase one will not be well done, and by contrast, in phase two, the temperature will rise too high.

According to the above arguments, the optimal excess air for the minimum and maximum loads is the maximum and minimum amount. At lower loads, reduced fuel and air supply leads to a lower flame height, which can cause incomplete heat transfer in the saturated liquid phase of the boiler. Increasing excess air under these conditions improves flame stability and heat distribution, ensuring adequate steam generation. Conversely, at higher loads, flame height and temperature are already sufficient, and additional excess air would reduce combustion temperature and efficiency, making minimal excess air more suitable. The results show that by augmenting the excess air from 0 to 25%, the gross power output reduces by about 2500 kW. Balancing combustion efficiency with power output involves setting excess air where gains from complete combustion offset losses from lower flame temperature and higher stack heat loss. At low loads, more excess air improves flame stability, while at high loads, minimal excess air preserves efficiency. Automated control with flue gas monitoring ensures optimal adjustment.

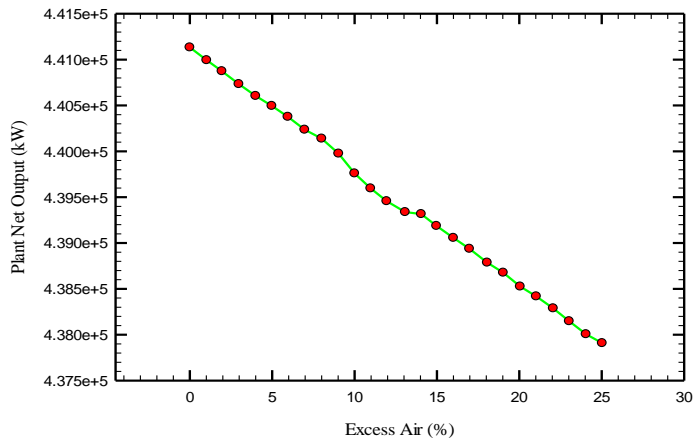


Figure 6. Variations of power plant net output with the percentage of excess air.

Figures 7 (a) and (b) present plant net electric efficiency variations and excess air plant's net heat rate. According to the illustrated explanations and results, the plant net electric efficiency decreases by increasing the excess air, and the plant net heat rate increases. The decreasing trend of net electrical efficiency and the

increasing trend of net heat rate in these figures are due to higher fuel consumption and auxiliary power requirements at increased loads. These conditions intensify cooling losses, thereby lowering the overall efficiency of the cycle.

These figures also display that the range of plant net electric efficiency changes is about 0.3%, and by increasing the excess air percentage from 0 to 25, the plant net heat rate enhances from 9069 to 9135 kJ/kWh. The fuel flow rate under normal conditions is equal to 86.97 t/h, and the pressure is supposed to be 1.5 bar according to the documentation of the Neka power plant. The above flow rate can be converted to the volume flow rate by considering the density of 0.8 kg/m³ for natural gas in standard conditions, equal to 108712.5 Nm³/h. Also, the calculated fuel consumption differs by approximately 1.5% from the reported value of the NEKA power plant (110,294 Nm³/h), which is within an acceptable margin of error.

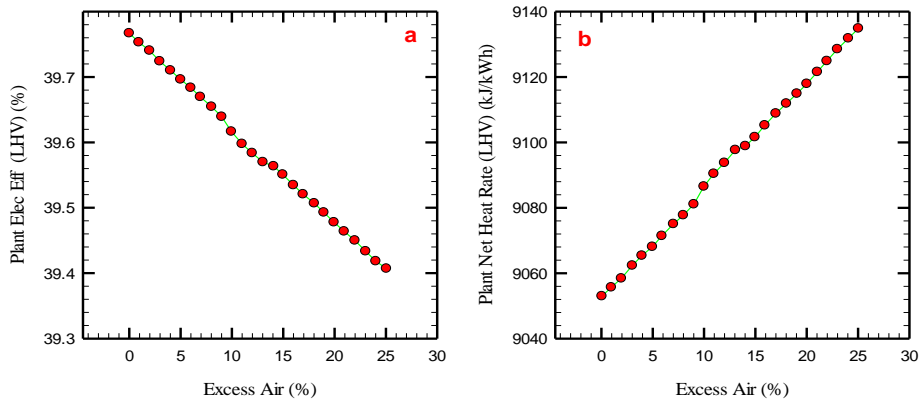


Figure 7. Effects of excess air on power plant (a) net electric efficiency and (b) net heat rate.

Power plant cycle conditions by removing heaters

Removing the heaters changes some parameters on the power plant cycle. The results are shown in Table 5.

Table 5. Results of removing heaters from power plant cycles.

Number of the removed heater (type)	Plant net output (KW)	Plant gross output (KW)	Plant gross electric efficiency (%)	Plant gross heat rate (kJ/kWh)
1 (low pressure water heater)	449092	438972	39.26	9170
2 (low pressure water heater)	449292	439185	39.28	9165
3 (low pressure water heater)	449777	439641	39.32	9156
4 (low pressure water heater)	449082	439027	39.26	9169

6 (high pressure water heater)	445399	435372	39.34	9151
7 (high pressure water heater)	476763	466196	39	8999

According to table 5, the following results are obtained.

Removing heaters 1, 2, 3, 4: removing these heaters reduces the power plant net power, gross power, gross electric efficiency, and gross heat rate and also enhances the fuel consumption very slightly. Therefore, neither technically nor economically, removing these heaters is not cost-effective.

Removing heater 6: the fuel consumption by eliminating this heater equals 86.07 t/h, reduced by about 1% compared to the standard condition. It seems that by removing this heater, due to the decrease in inlet fluid temperature into the boiler and the constant condition of the outlet from the boiler, the fuel flow rate should be increased, which in practice, the same condition occurs. But in the simulation, due to the consideration of thermal equilibrium of cycle simultaneously, by removing this heater, the inlet vapor flow rate into the heater 7 increases significantly, which causes the compensation of the reduced temperature. Hence the fuel flow rate reduces slightly. Removing this heater reduces net power, gross power, gross electric efficiency, and gross heat rate but slightly enhances fuel consumption. Due to the slight reduction in fuel consumption, removing this heater is not cost-effective, neither technically nor economically.

Removing heater 7: the fuel consumption by eliminating this heater is equal to 90.64 t/h, which has been increased by about 4% compared to the standard condition. The simulation results show that removing this heater augments the power plant's net power and gross power by 5.36% and 5.4%, respectively. It is because of passing a higher flow rate through the H.P. turbine. So removing this heater enhances the output power but increases the fuel consumption, causing the efficiency to be reduced. Removing this heater results in 30 degrees Celsius lower temperature at the inlet water of the boiler, which leads to higher thermal tensions and depreciation in the boiler. Consequently, removing this heater is also not cost-effective. It is noteworthy that this heater is removed from the circuit to increase output power during the peak times of the summer due to the higher electricity demand. Removing heaters can provide short-term output gains by increasing turbine mass flow, but it also raises fuel use, reduces efficiency, and increases thermal stresses on boiler components. Prolonged operation under these conditions accelerates wear, increases maintenance costs, and undermines long-term plant.

Sea temperature

Figures 8 (a) and (b) present the variations of plant gross and net output and plant gross and net electric efficiency with sea temperature, respectively. These figures demonstrate that the sea temperature changes affect the output power and efficiencies. Rising sea temperature reduces condenser cooling efficiency, which increases steam turbine back pressure and leads to a decline in plant output and efficiency. These impacts can be mitigated by increasing cooling water flow during warm periods, integrating hybrid seawater–air cooling systems, and employing advanced heat exchanger materials to enhance heat transfer. As a result, fuel consumption significantly as for one degree of rising seawater temperature, the plant output power and cycle efficiency decrease by 1459 kW and 0.156%, respectively. Integrating real-time environmental monitoring with predictive control enables proactive adjustment of cooling, combustion, and operational parameters in response to ambient and sea temperature changes. This approach can improve efficiency, maintain stable output, and mitigate the negative effects of thermal variations on plant performance.

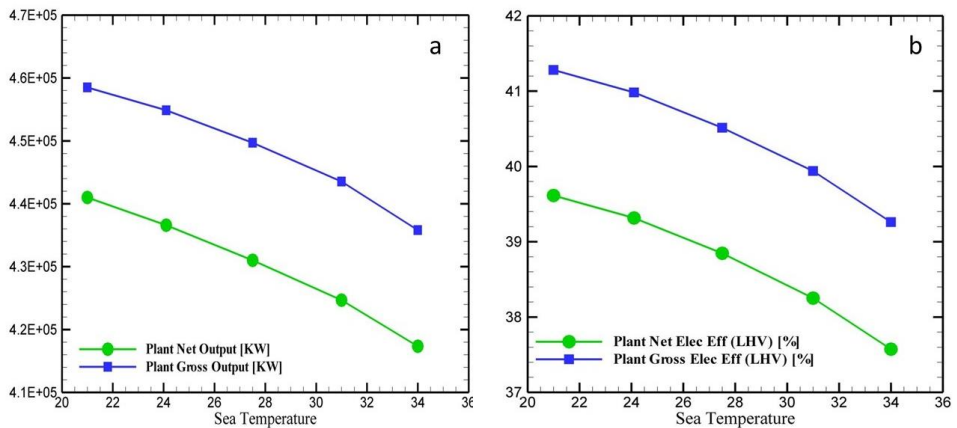


Figure 8. Effects of sea temperature on power plant (a) gross and net output and (b) gross and net efficiency.

Conclusion

This paper presented a comprehensive energy and exergy analysis of Neka's combined cycle power plant (4×440 MW, total capacity 1,760 MW) using Thermoflow simulations under both minimum (220 MW) and maximum (440 MW) load conditions. The effects of different parameters, including the outlet water sub-cooled temperature of condenser, ambient temperature, excess air, removing heaters, and sea temperature on power plant gross and net output

and gross and net electric efficiency are evaluated. The findings indicated that the boiler is the main source of exergy destruction, primarily due to combustion irreversibility and stack losses, with notable contributions from the condenser and heaters. Increasing the sea temperature by 6 °C diminished plant output and cycle efficiency by 1,459 kW and 0.156%, respectively, but an increase in an excess air from 0% to 25% resulted in a reduction of gross power by approximately 2,500 kW. Furthermore, the analysis of heater removal revealed immediate improvements in output, although also elicited apprehensions over long-term viability, highlighting the compromises between operating efficiency and durability.

This analysis provides practical insights into optimizing power plant operation under variable environmental conditions through careful management of combustion parameters, cooling strategies, and load distribution. The methodology and results of this study can be extended to similar power plants in Iran and worldwide to improve efficiency and reliability. Future research should focus on integrating advanced optimization algorithms, predictive control systems, and real-time monitoring to further enhance performance and adaptability of combined cycle plants under dynamic operating environments.

Disclosure statement and funding

The authors declare no potential conflicts of interest. The present study received no financial support from any organization or institution.

Acknowledgment

2023 Provincial Higher Vocational Education Teaching Reform Research and Practice Project: "Construction and Research of a Course Package System for New Engineering Professional Clusters from the Perspective of Integration of Specialization and Innovation- A Case Study of Automation Related Majors (2023JG398)"

References

- [1] Ibrahim, T. K., Mohammed, M. K., Awad, O. I., Abdalla, A. N., Basrawi, F., Mohammed, M. N., Najafi, G., & Mamat, R. (2018). A comprehensive review on the exergy analysis of combined cycle power plants. *Renewable and Sustainable Energy Reviews*, 90, 835–850. <https://doi.org/10.1016/j.rser.2018.03.072>
- [2] Hosseini, M., Afrouzi, H. H., Arasteh, H., & Toghraie, D. (2019). Energy analysis of a proton exchange membrane fuel cell (PEMFC) with an open-ended anode using agglomerate model: A CFD study. *Energy*, 188, 116090. <https://doi.org/10.1016/j.energy.2019.116090>

- [3] Ahmadi, B., Golneshan, A. A., Arasteh, H., Karimipour, A., & Bach, Q.-V. (2020). Energy and exergy analysis and optimization of a gas turbine cycle coupled by a bottoming organic Rankine cycle. *Journal of Thermal Analysis and Calorimetry*, 141, 495–510. <https://doi.org/10.1007/s10973-019-09088-6>
- [4] Li, K., Chi, J., & Zhang, S. (2023). Energy and exergy analysis of gas turbine combined cycle with exhaust gas recirculation under part-load conditions. *Journal of Mechanical Science and Technology*, 37(5), 2149–2160. <https://doi.org/10.1007/s12206-023-2102-1>
- [5] Mokhtari, H., Esmaili, A., & Hajabdollahi, H. (2016). Thermo-Economic Analysis and Multiobjective Optimization of Dual Pressure Combined Cycle Power Plant with Supplementary Firing. *Heat Transfer—Asian Research*, 45(1), 59–84. <https://doi.org/10.1002/htj.21153>
- [6] Ahmadi, G. R., & Toghraie, D. (2016). Energy and exergy analysis of Montazeri Steam Power Plant in Iran. *Renewable and Sustainable Energy Reviews*, 56, 454–463. <https://doi.org/10.1016/j.rser.2015.11.074>
- [7] Pattanayak, L., Sahu, J. N., & Mohanty, P. (2017). Combined cycle power plant performance evaluation using exergy and energy analysis. *Environmental Progress & Sustainable Energy*, 36(4), 1180–1186. <https://doi.org/10.1002/ep.12546>
- [8] Ali, M. S., Nawaz, S. Q., Dileep, K., Summeet, K., & and Kumar, S. (2020). Energy and exergy analysis of a 747-MW combined cycle power plant Guddu. *International Journal of Ambient Energy*, 41(13), 1495–1504. <https://doi.org/10.1080/01430750.2018.1517680>
- [9] Aliyu, M., AlQudaihi, A. B., Said, S. A. M., & Habib, M. A. (2020). Energy, exergy and parametric analysis of a combined cycle power plant. *Thermal Science and Engineering Progress*, 15, 100450. <https://doi.org/10.1016/j.tsep.2019.100450>
- [10] Omidpanah, M., Elomee, S. A. A., & Ashtian Malayer, M. (2021). Process Simulation and Extraction of Parameters Affecting the Production Capacity and Efficiency of a Combined Cycle Power Plant Unit (Case study: Yazd Combined Cycle Power Plant). *Karafan Journal*, 18(3), 55–77. <https://doi.org/10.48301/kssa.2021.130679>
- [11] Anetor, L. E., O. E., & and Odetunde, C. (2022). Classical and advanced exergy-based analysis of a 750 MW steam power plant. *Australian Journal of Mechanical Engineering*, 20(2), 448–468. <https://doi.org/10.1080/14484846.2020.1716509>
- [12] Altarawneh, O. R., Alsarayreh, A. A., Al-Falahat, A. a. M., Al-Kheetan, M. J., & Alrwashdeh, S. S. (2022). Energy and exergy analyses for a combined cycle power plant in Jordan. *Case Studies in Thermal Engineering*, 31, 101852. <https://doi.org/10.1016/j.csite.2022.101852>
- [13] Elwardany, M., Nassib, A. M., Mohamed, H. A., & Abdelaal, M. R. (2023). Energy and exergy assessment of 750 MW combined cycle power plant: A case study. *Energy Nexus*, 12, 100251. <https://doi.org/10.1016/j.nexus.2023.100251>
- [14] Omara, A. A. M., Mohammedali, A. A. M., & Dhivagar, R. (2024). Energy, exergy and advanced exergy analyses on Garri “1” combined cycle power plant of Sudan.

- International Journal of Thermofluids*, 24, 100930.
<https://doi.org/10.1016/j.ijft.2024.100930>
- [15] Prakash, D., & Singh, O. (2024). Exergy analysis of combined cycle power plant with carbon capture and utilization. *Energy Sources, Part A: Recovery, Utilization, and Environmental Effects*, 46(1), 15297–15318.
<https://doi.org/10.1080/15567036.2020.1810827>
- [16] Abdulsitar, A. S., Saeed, A. F., & Ismaeel, H. H. (2025). Performance Evaluation of a 1500 MW Combined Cycle Power Plant using Energy and Exergy Analysis. *Journal of Advanced Research in Fluid Mechanics and Thermal Sciences*, 128(1), 123–150. <https://doi.org/10.37934/arfmts.128.1.123150>
- [17] Reza Babaei, M. M., Mohsen Kiamansouri, Milad Khanchoupan, Elham Moghadamnia. (2025). Investigating the effect of environmental conditions and fuel type on the energy and exergy parameters of a steam power plant. *Journal of Science and Technology in Mechanical Engineering*, 3(2).
<https://doi.org/10.22034/stme.2025.482810.1083>
- [18] Ibrahim, T. K., Rahman, M., Mohammed, M., & Basrawi, F. (2016). Statistical analysis and optimum performance of the gas turbine power plant. *International Journal of Automotive and Mechanical Engineering*, 13(1), 3215–3225. <https://doi.org/10.15282/ijame.13.1.2016.8.0268%20%20>
- [19] Ibrahim, T. K., Rahman, M. M., Ali, O. M., Basrawi, F., & Mamat, R. (2016). Optimum Performance Enhancing Strategies of the Gas Turbine Based on the Effective Temperatures. *MATEC Web of Conferences*, 38, 01002.
<https://doi.org/10.1051/matecconf/20163801002>
- [20] Kazemian, M. E., & Gandjalikhan Nassab, S. A. (2020). Thermodynamic Analysis and Statistical Investigation of Effective Parameters for Gas Turbine Cycle using the Response Surface Methodology. *International Journal of Engineering*, 33(5), 894–905. <https://doi.org/10.5829/ije.2020.33.05b.22>
- [21] Alnaimi, F. B. I., Jasbeer Singh, M. S., Al-Bazi, A., Al-Muhsen, N. F. O., Mohammed, T. S., & Al-Hadeethi, R. H. (2021). Parametric investigation of combustion process optimization for Gas Turbines at SJ Putrajaya. *Energy Reports*, 7, 5722–5732. <https://doi.org/https://doi.org/10.1016/j.egvr.2021.08.202>
- [22] Wang, Z., Duan, L., & Zhang, Z. (2022). Multi-objective optimization of gas turbine combined cycle system considering environmental damage cost of pollution emissions. *Energy*, 261, 125279.
<https://doi.org/https://doi.org/10.1016/j.energy.2022.125279>
- [23] Elwardany, M., Nassib, A. M., & Mohamed, H. A. (2024). Exergy analysis of a gas turbine cycle power plant: a case study of power plant in Egypt. *Journal of Thermal Analysis and Calorimetry*, 149(14), 7433–7447.
<https://doi.org/10.1007/s10973-024-13324-z>
- [24] Kamali, K., Barghi Jahromi, M. S., & Sefid, M. (2022). Energy and Exergy Analysis of a Direct Solar Steam Power Plant with Solar Parabolic Concentrator for Yazd City with Several Water Preheaters. *Karafan Journal*, 19(1), 333–355.
<https://doi.org/10.48301/kssa.2021.287183.1540>
- [25] Documentation of Shahid Salimi Neka Power Plant.
- [26] Ameri, M., Ahmadi, P., & Hamidi, A. (2009). Energy, exergy and exergoeconomic analysis of a steam power plant: A case study. *International Journal of energy research*, 33, 499–512. <https://doi.org/10.1002/er.1495>